Indian Journal of Geo Marine Sciences
Vol. 48 (07), July 2019, pp. 1070-1080

Time of arrival estimation using fast Fourier transform overlap for underwater distance measurement

Chee Sheng Tan, Rosmiwati Mohd-Mokhtar*, & Mohd Rizal Arshad

Underwater Control Robotics Research Group, School of Electrical and Electronic Engineering
Universiti Sains Malaysia, Engineering Campus
14300 Nibong Tebal, Seberang Perai Selatan, Pulau Pinang, Malaysia

*[E-mail: eerosmiwati@usm.my]

This paper presents an underwater acoustic distance measurement system based on Fast Fourier Transform (FFT) overlap. The low-cost underwater communication device is developed to achieve the objective. The time-of-arrival (TOA) technique is used to estimate the distance between the transmitter and receiver. The TOA estimation is derived based on the intensity of the received signal with frequency of interest. The extraction of the signal from the receiver is performed by using digital signal processing algorithms. FFT is used to convert the receiving signal from time domain into frequency domain for extracting the information of signal (relevant frequency and amplitude). Hence, TOA estimation can be obtained from the frequency information using overlap transform processing. This enables the increase of the TOA measurement resolution with the overlap technique. Trilateration algorithm is also employed as to determine the relative position of underwater target based on distance measurement. This approach is tested on shallow underwater to estimate the position of target. The experimental results are presented to demonstrate its capabilities.

[Keywords: Underwater acoustic distance measurement; Fast Fourier Transform (FFT) overlap; Time-of-arrival; Digital signal processing; Trilateration]

Introduction

Underwater acoustics is a study of sound in the water that encompass not only about sound propagation, but also the masking of sound signals by the interfering phenomenon. It also includes study of signal processing for extracting these signals from interference[1,2]. Underwater acoustic uses sound to learn about the physical and biological characteristics of the lake, river or sea. Acoustic wave propagates better than electromagnetic wave in underwater applications[3]. This is because the transmission of electromagnetic wave suffers from strong attenuation under water. Underwater acoustic is a very important vector in underwater communication system, localization system and positioning system[4,5,6].

Underwater distance measurement using sonar has been widely used in environment monitoring, obstacle avoidance system and underwater object detection[7,8]. Sonar transducer, also known as ultrasonic sensing, is a device used for extracting the information by using propagation of acoustic energy[9]. Commonly, the frequencies are in the range of 20 kHz to 100 kHz. Sonar is typically mounted on an autonomous surface vessel (ASV) or an autonomous underwater vehicle (AUV) to detect underwater objects. The higher frequency of ultrasonic leads to higher accuracy of the distance measurement. However, high ultrasonic frequency works only at short range[10].

Generally, the distance between transmitter and receiver using ultrasonic sensor is measured based on time-of-arrival (TOA)[11,12,13] and time-different-of-arrival (TDOA)[14,15,16]. TOA measurement requires time synchronization between transmitter and receiver. The measured distance is determined based on a set of circles. On the other hand, TDOA estimation is typically obtained by intersection of multiple hyperbolic curves. TDOA only requires time synchronization among the receivers since it does not utilize the transmission time from the transmitter.

There are two common methods that normally being used to estimate TOA, namely, threshold method and cross-correlation method[17]. The threshold method can be considered as the simplest among these two techniques; however, it has poor accuracy of estimation. On the other hand, cross-correlation method gives a more accurate estimation than threshold, but it requires both transmitting signal and receiving signal to measure the time lag. Thus, the complexity increases.

Pinger is an acoustic transmitter which produces ultrasonic pulses to transmit a signal continuously[18]. Pinger is often installed on AUV to determine the range measurement by emitting the signal. It is also placed under the bottom of the sea floor to be used as a directional beacon. For military application, pinger can act as a bait to send false signal to enemy ships and submarines. On the other hand, hydrophone is an acoustic receiver that can detect and record signal under water. Most hydrophones are able to produce small electrical current when subjected to changes in underwater pressure[19]. It is able to measure ocean sounds by amplifying and recording the electrical signals. Hydrophone is often used for tracking divers, submarines and underwater targets.

Most of underwater acoustic communication requires use of high cost hardware devices. This is to ensure accurate distance measurement in addition to coping with the noise and dynamic changes of the underwater environment. The high cost constraint limits the research activities within this field. Due to this factor, there is a need to develop a low-cost underwater communication device which provides good performance to achieve the objectives.

The aim of this project is to develop a low-cost design of an underwater hydrophone and pinger. The system includes sensors, signal conditioning circuits and digital signal processing. In this study, the fast Fourier transform (FFT) overlapping method is proposed to estimate the TOA for underwater distance measurement. The signal with frequency of interest is selected using FFT. The timing when its magnitude reaches maximum is determined as TOA. An algorithm is developed to perform FFT processing with low latency.

Approach and Methods

Pinger and hydrophone

In this approach, piezoelectric is the most suitable material to be used for underwater communication due to the high acoustic impedance matching with water[20]. Therefore, a custom made pinger is built by using piezoelectric disc as shown in Figure 1(a). Piezoelectric materials have been used in underwater acoustic transducers since 1917. Paul Langevin, a French physicist, had developed an underwater acoustic transducer by using piezoelectric crystal to detect submarines[21].

An acoustic hydrophone with commercial version used for underwater application generally costs around USD 1000[22,23]. Nowadays, there is also available in the market a cheaper hydrophone, Aquarian Audio H2a. This hydrophone which is omni-directional has a range of detection of less than 80 m[24]. Another low-cost small hydrophone is shown in Figure 1(b). Both pinger and hydrophone are waterproof which can be placed in shallow water.

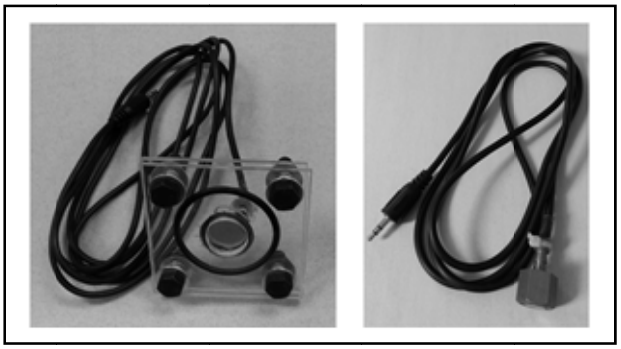

(a) (b)

Fig. 1 — Underwater transducers (a) Pinger and (b) Hydrophone

Signal transmitting and receiving circuits

In this project, transmitter circuit is the first to be designed for amplifying the input signal. To drive the piezoelectric disc, an external drive circuit with a transistor is used. The inductor coil will store energy during the oscillations and magnify the signal with appropriate output peak-to-peak voltage. As a result, acoustic wave is produced when there is a vibration of the metal plate due to the voltage across the piezoelectric disc. Microcontroller will generate a square wave signal at the selected frequency with 50% duty cycle.

Basically, the receiver circuit is divided into four parts. The first part is a preamplifier circuit, which is built to increase the low-level acoustic signal to line level[25]. Then, these oscillations are amplified by a factor of desired gain. A high-pass filter is designed to attenuate frequencies below its cut-off frequency or noises. Otherwise, a narrow high-order band-pass filter with multiple feedback or Sallen-Key is used to reject all signals outside the interested frequency. The last part is an analog-to-digital converter (ADC) that converts an analog input signal from filter circuit into digital form. High sampling rate of ADC can sample signal at high frequency, but it may result in high cost.

To reduce the cost, the receiver circuit will only include a preamplifier circuit which is operating at ± 9 V. A sound card is used to interface between

the receiver circuit and microcontroller. It contains ADC to digitize analog signal received and can support sampling rate up to 96 kHz. A real time clock (RTC) is used to keep the current time for microcontroller due to no network connection.

According to Figure 2, the hardware is built around the system using two microcontrollers. They are used as the main control unit for the transmitter and receiver accordingly. The microcontrollers are connected to the router for network communication. This system is designed and built to measure the distance measurement without direct contact between transmitter and receiver modules.

Digital signal processing

Pulse code modulation (PCM) is digital audio processing which converts an analog signal into digital signal. First, the magnitude of the analog continuous signal is sampled at regular time intervals. Then, it is quantized to binary code in digital form. The resolution is supported by sampling rate and the bit depth[26]. Mostly sound cards have internal ADC that can read and write PCM data directly.

Fast Fourier transform is an efficient implementation of the transformation to convert the acoustic signal from time domain into frequency domain and vice versa[27]. It is numerically efficient method to reduce the computation time required to calculate discrete Fourier transform (DFT). The applications of FFT algorithms are linear filtering, correlation and spectrum analysis.

Fast Fourier transform was originally developed by Gauss in 1805. However, his work did not analyze the asymptotic computational time. The FFT algorithm became popular after a paper was published in 1965 by Cooley and Tukey[28]. This is because the algorithm reduces the number of complex multiplications compared to DFT. The DFT of discrete N-point sequence $x(n)$ is denoted by $X(k)$ as in (1).

$$X(k) = \sum_{n=0}^{N-1} x(n)\omega_N^{nk} \quad \ldots (1)$$

where $\omega_N = e^{-j2\pi/N}$ is a primitive root of unit and $0 \le k \le N-1$. The direct evaluation of DFT requires N^2 complex multiplications and $N(N-1) \cong N^2$ complex addition to obtain a complete set of its coefficients. If the value of N is larger than the number of computations, the value is unacceptable in practice. On the other hand, FFT algorithm using the formula requires $N \log_2 N$ complex multiplications and addition operations.

The FFT overlap can be used to increase the accuracy of TOA in time series. The higher the percentage of overlapping the higher is the time resolution. Unfortunately, the computation load for processing FFT will be higher. Figure 3(b) shows the 50% FFT overlap corresponding to 0, N/2, N etc. Hence, the TOA accuracy is increased by 50% as compared to Figure 3(a) which has no overlap. On the other hand, 100% FFT overlap is the highest accuracy

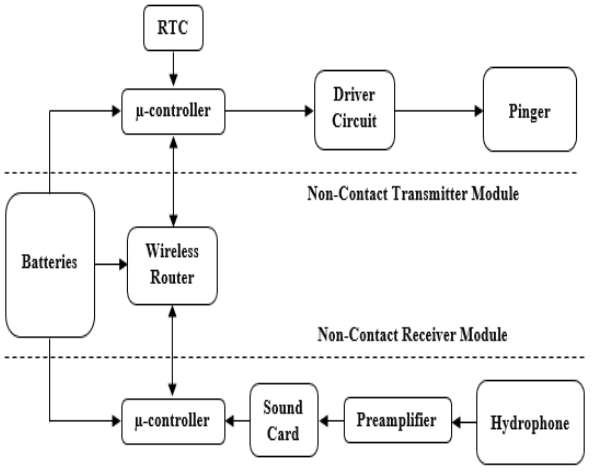

Fig. 2 — Structure of hardware control system

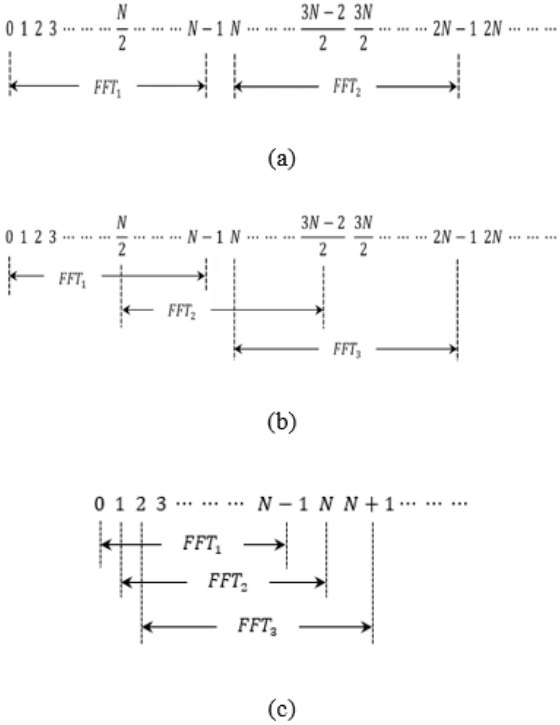

Fig. 3 — Data string in time series (a) No FFT overlap, (b) 50% FFT overlap, and (c) Fully FFT overlap

due to the fixed width of consecutive samples that undergo FFT. TOA is the time travelled of an acoustic signal from pinger to hydrophone. This value can be estimated using equation (2) after the signal is computed by forward FFT:

$$TOA = \frac{N}{kF_S}\left(N_{FFT} - 1\right), k = \begin{Bmatrix} 1, no\ overlap \\ 2, 50\ \%\ overlap \\ 4, 75\ \%\ overlap \\ N, 100\ \%\ overlap \end{Bmatrix} \quad \ldots (2)$$

where F_S is sampling rate, N is length of FFT, N_{FFT} is position number of FFT which is detected at maximum amplitude and k is the value that depends on the type of overlap percentages for FFT. The speed, s of an acoustic wave propagates in distilled and sea water are approximately 1484 m/s and 1531 m/s, respectively, at room temperature. The distance, d can be calculated using equation (2) and (3) to form (4).

$$d = s \times TOA \quad \ldots (3)$$

$$d = \frac{sN}{kF_S}\left(N_{FFT} - 1\right) \quad \ldots (4)$$

Trilateration

The most common method for positioning is trilateration which estimates the position of underwater targets by distance measurement[29]. This process mostly depends on TOA value of acoustic signal from sensors. It measures the arrival time with distance calculation to estimate the position of underwater target. The principle of trilateration is illustrated in Figure 4. The relative distances correspond to the travel time at propagation speed of the signal.

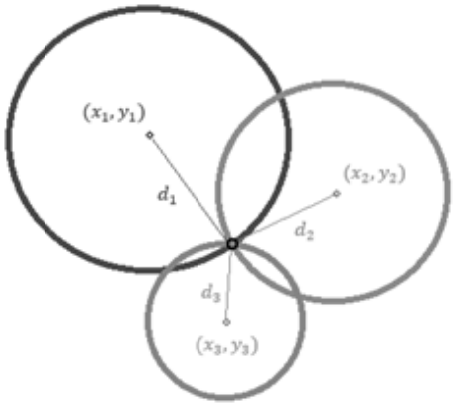

Fig. — 4 Trilateration

Consider only two points (x_1, y_1) and (x_2, y_2) are known, two equations are obtained based on trilateration as in (5) and (6),

$$(x - x_1)^2 + (y - y_1)^2 = {d_1}^2 \quad \ldots (5)$$

$$(x - x_2)^2 + (y - y_2)^2 = {d_2}^2 \quad \ldots (6)$$

Assume two hydrophones are located at (0, 0) and (x_2, 0), the position x and y can be calculated using equation (7) and (8):

$$x = \frac{{d_1}^2 - {d_2}^2 + {x_2}^2}{2x_2} \quad \ldots (7)$$

$$y = \sqrt{{d_1}^2 - x^2} \quad \ldots (8)$$

where $x_2 > 0$.

Target source positioning process

The flow chart for the algorithm to determine position of target is shown in Figure 5. A continual stream of sounds is recorded by hydrophone. Each segment is extracted from the signal and taken for FFT overlap processing. The frequency of interest is

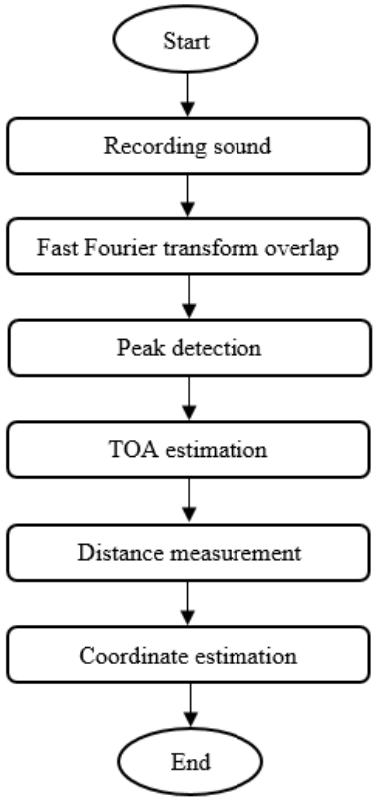

Fig. 5 — Flow chart of positioning system

selected based on the frequency that contains as similar a transmitted signal. If the amplitude of selected frequency is above the threshold value in frequency domain, the segmented signal can be considered as maximum value that is related to frequency of interest. Then, local maximum can be found among these maximum values after all the segmented signals are processed repeatedly by FFT overlap.

The delay time can be obtained after the frequency information is extracted from the signal. The delay time represents the TOA between the hydrophone and the target source. The coordinate of the target (x, y) is determined by using multi-lateration technique. The locations of hydrophones with the distance among the relative location of points are considered in calculation to estimate the position of sound source.

Results and Discussion

Received signal strength testing

The intensity measurement of received signal based on FFT technique is carried out in air as shown in Figure 6. The distance between transmitter and receiver is varied from 1 m to 15 m. According to Nyquist theorem, the highest signal frequency should be less than twice the sampling rate in the PCM so that the original information cannot be reconstructed at the hydrophone which might not lead to aliasing. Thus, the interested frequency should be at the range below 24 kHz. 18 kHz is selected to be emitted continuously by pinger since the resonant frequency of hydrophone is 18 ± 2 kHz.

(a) (b) (c)

Fig. 6 — Experimental set-up of received signal strength (a) 1 m, (b) 5 m, and (c) 10 m

Figure 7 shows the results of the experiment. The surrounding noise signal at 18 kHz is detected at -8 dB. The results clearly show that the hydrophone can detect the acoustic signal up to 15 m from the source in air. However, the detected signal beyond 10 m is frustrated in the range of ±1 dB. According to the trend, distance can be calculated using equation (9),

$$x = e^{\frac{28.634 - y}{9.242}} \quad \ldots (9)$$

where x is distance in meters and y is intensity in dB. This measurement is accurate within 10 m. The signal intensity decreases as the distance increases.

TOA measurement based on FFT overlap technique

The input signal is generated and recorded in air environment as shown in Figure 8. The distance

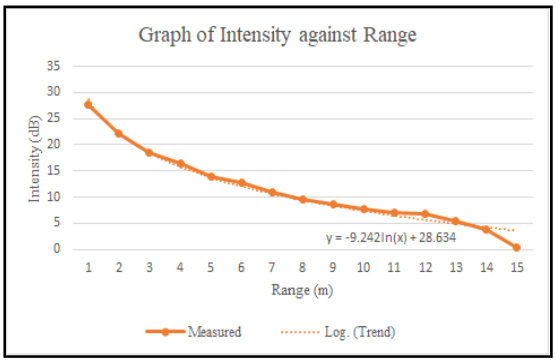

Fig. 7 — Results of intensity measurement at 18 kHz

Fig. 8 — Experiment set-up in air

between transmitter and receiver is set around 3.1 m for this test. This experiment is to prove that low-cost platform is able to provide accurate TOA estimation based on FFT overlap. The deployed TOA is calculated as 9.04 ms, where the speed of sound in air is 343 m/s.

The whole signal is sampled using sampling rate of 96 kHz within a period of 0.1 s (9600 samples). The frequencies of the base signals (without noise) are generated as 17 kHz, 18 kHz and 19 kHz (Fig. 9) since the resonant frequency of hydrophone is 18 ± 2 kHz. They are continuously emitted for 0.01 s by pinger. An algorithm for setting up parameters for receiving and processing signal is shown in Table 1.

A segment length (N=1024 points) of signal is processed by FFT to divide into frequency components. Each segment that contains the frequency value (17 kHz, 18 kHz and 19 kHz) is selected throughout the frequency spectrum. The amplitude of the selected frequency value that is greater than threshold value is chosen. The process is repeated for each segment to figure out the maximum amplitude.

In the first experiment, the percentage of overlap is varied from 0%, 50% and 75% to demonstrate the accuracy of TOA. The experiment is tested on the signal from Figure 9(a). No overlap processing only transforms 9600 samples of signal into 9 segments. However, the result demonstrated that the delay time is estimated within the range between 0 and 21.34 ms. It provides unknown value of result which led to inaccuracy of reading.

On the other hand, the accuracy of TOA is increased when the signal is processed by 50% overlap. It further increased the accuracy if the signal is computed by 75% of FFT overlap. The TOA estimation is between 8 and 13.34 ms that substantially reduced the error. The overall result of TOA estimation using different percentage of overlap is shown in Figure 10. Based on the result shown in Table 2, it indicates that the higher percentage of overlapping processing results in the higher accuracy of delay time.

The second experiment is carried out based on 100% FFT overlap and this algorithm is tested on three different recording signals as shown in Figure 9. The result is shown in Figure 11. The result shows that the maximum amplitude of frequency 17 kHz is at position 885 according to Figure 11(a), the maximum amplitude of frequency 18 kHz is at position 861 according to Figure 11(b) and the maximum amplitude of frequency 19 kHz is at position 919 according to Figure 11(c). Figure 12 shows the result of TOA by using equation (2). The actual TOA is 0.00904 s which means that the

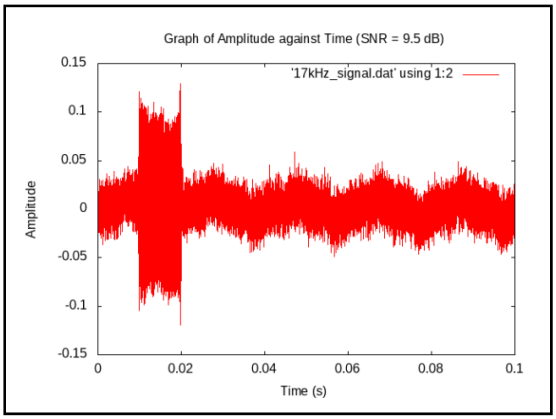

(a)

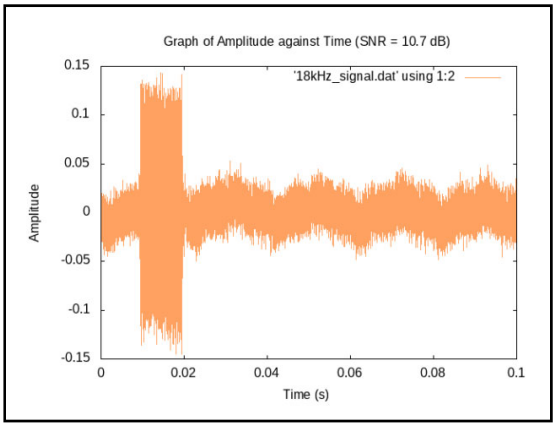

(b)

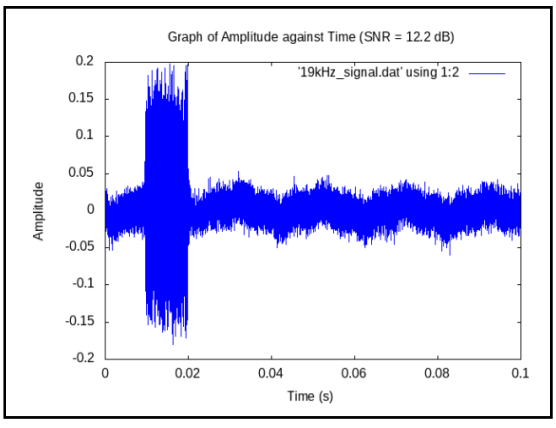

(c)

Fig. 9 — Signal recorded in real environment with noise (a) 17 kHz, (b) 18 kHz, and (c) 19 kHz

Table 1 — Parameters set-up

DSP	Parameters	Settings
PCM	Interface	hw: 0
	Sample Rate	96000 bits/second
	Buffer Size	960 frames
FFT	Direction	Forward
	FFT Length	1024 frames
	Overlap	0%, 50%, 75%, 100%

Table 2 — Experimental results of TOA based on different percentage of FFT overlap

Overlap (%)	N_{FFT}	TOA (millisecond)
0	2	10.67 ± 10.67
50	3	10.67 ± 5.33
75	5	10.67 ± 2.67

estimation error of the system is less than 5.88%. Hence, the proposed FFT overlap can provide almost accurate TOA estimation. This is because the frequency of interest can be easily be identified by using this algorithm.

Experimental test of distance measurement

The distance measurement by using proposed FFT overlapping technique is carried out in this experiment. The frequency of signal emitted from transmitter is 18 kHz. Eighteen pulses of signal are transmitted since the range of distance between pinger and hydrophone is small. Consequently, low intensity of signal is emitted to determine the magnitude of the received signal.

In this experiment, 64 points of short length are passed by FFT using the 100% overlap. The sampling rate is set as 48 kHz. The receiver is moved incrementally for a certain distance at 10 cm interval. Five consecutive measurements are taken for each distance. Both transmitter and receiver modules are started at the same time. The measured distance can be determined using equation (4). The experimental results for the distance measurement are shown in Table 3.

Figure 13 shows the result of distance measurement by comparing measured distance versus actual distance. It is clearly shown that there is an error in the measured distance as compared to the actual distance. The percentage error is significantly large at the shortest distance between transmitter and receiver. The longer distance gives smaller error. The experimental result indicated that within appropriate distance of the receiver and the transmitter, the proposed method can measure the distance correctly.

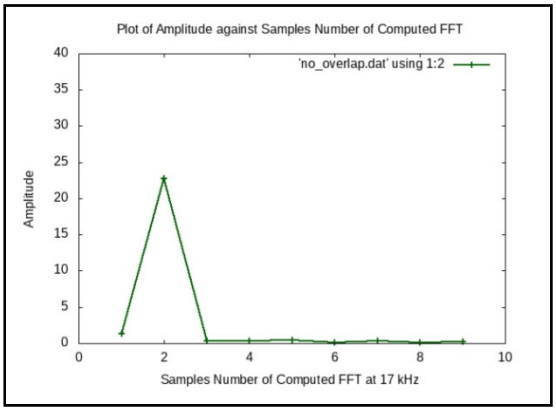

(a)

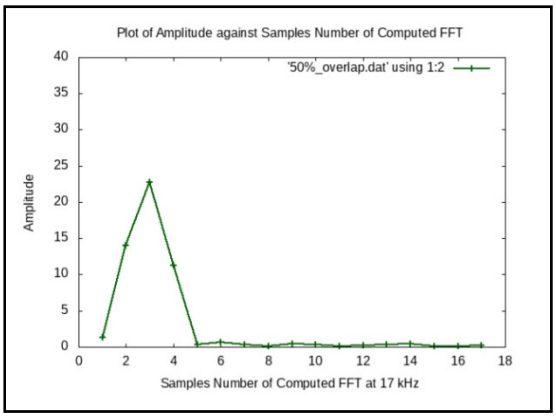

(b)

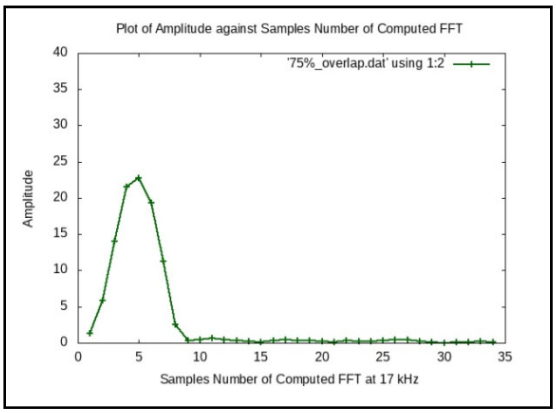

(c)

Fig. 10 — Peak detection (number of computed FFT at 17 kHz) (a) 0%, (b) 50%, and (c) 75%

The second experiment is conducted in a mini aquarium as shown in Figure 14. This experiment is done to ensure the platform can work well in water condition. The samples are taken autonomously every 1 min, and the data are collected from 10 samples. For short range distance measurement, the overall processing time for each sample is merely 0.2 s.

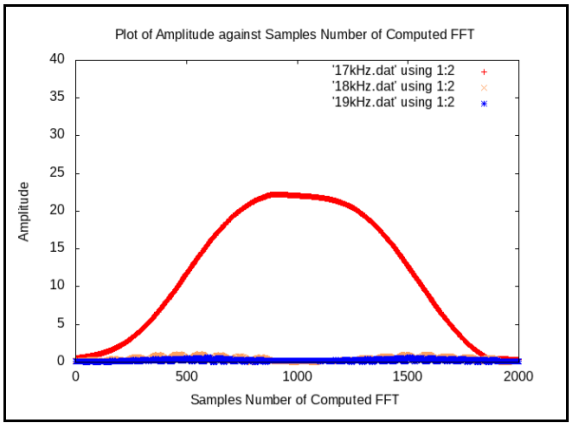

(a)

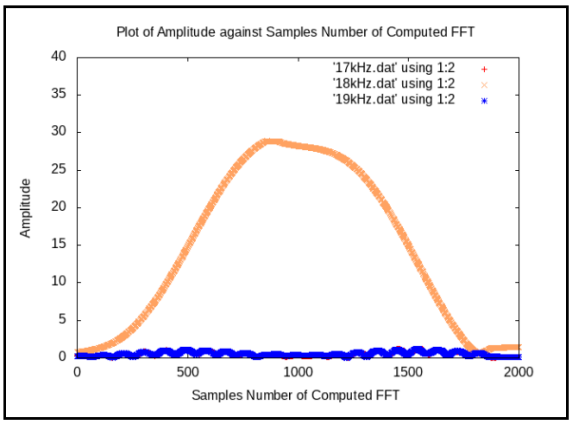

(b)

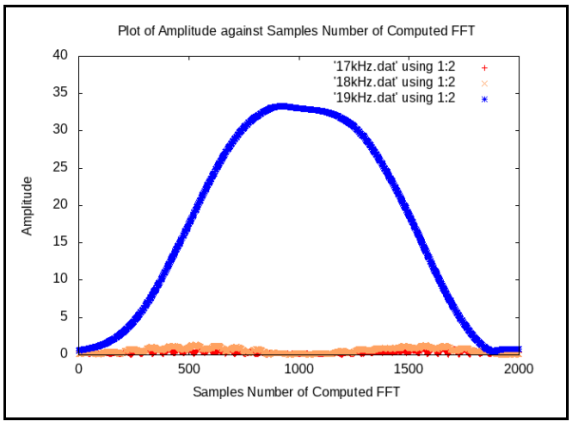

(c)

Fig. 11 — Results of proposed FFT overlap

```
_____FFT Overlap_____
17 kHz : max(N_FFT) = 885 th, TOA = 0.009208 s

18 kHz : max(N_FFT) = 861 th, TOA = 0.008958 s

19 kHz : max(N_FFT) = 919 th, TOA = 0.009563 s
```

Fig. 12 — Results of TOA estimation

Table 3 — Experimental results of distance measurement using FFT overlap

Actual Distance (cm)	TOA (msec)	Measured Distance (cm)	Error (%)
10	0.542	18.58	85.80
20	0.813	27.87	39.35
30	1.021	35.01	16.70
40	1.333	45.73	14.33
50	1.563	53.59	7.18
60	1.875	64.31	7.18
70	2.125	72.89	4.13
80	2.438	83.61	4.51
90	2.688	92.18	2.42
100	3.000	102.90	2.90

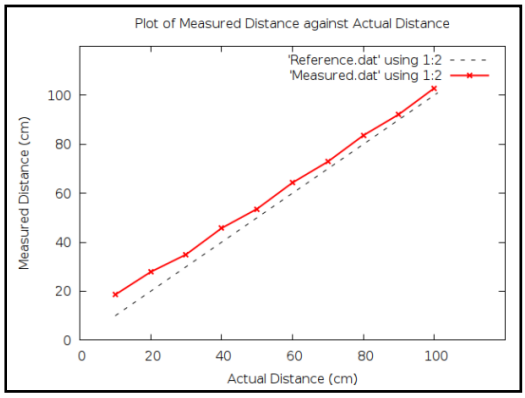

Fig. 13 — Plot of measured distance versus actual distance

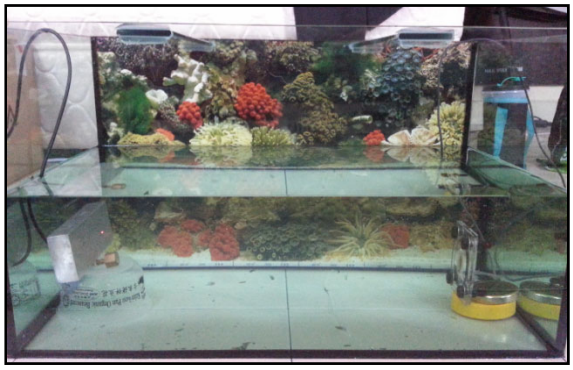

Fig. 14 — Experimental set-up of distance measurement in water

According to Figure 15, FFT_N is N number of computed FFT, F is frequency at specific bin and M is magnitude in frequency domain. The result shows that the maximum amplitude at 18 kHz is on the position of FFT_{17}. However, there is an obstacle or a wall behind the hydrophone which may influence the results. The distance between the wall and hydrophone is 8 cm. It is clearly shown that the hydrophone detects the reflected signal from the wall as shown in Figure 15.

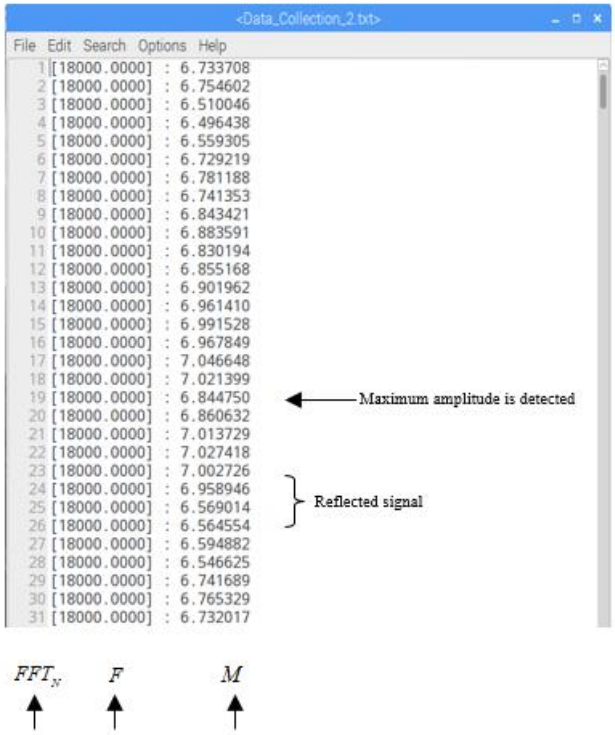

Fig. 15 — Data collection in text file

By assuming that *s* is 1484 m/s and N_{FFT} is 17, the measurement result is calculated as 0.495 m; whereas the actual distance is 0.45 m, which means that the measurement error of the system is 10%. It is observed that the hydrophone can detect the signal from pinger with small measurement error in water.

Experimental test of position estimation

The proposed algorithm is implemented for TOA estimation in this experiment. The transmitter module consists of pinger and is placed under the pool at around 2.2 m depth. The hydrophones are placed at 3 m as shown in Figure 16. The signals from left hydrophone, H_1 and right hydrophone, H_2 are recorded at the same time. The frequency of signal emitted from pinger is 16.5 kHz for 0.01 s. The emission and recoding of signal is done autonomously.

Similarly, a segment length (*N*=1024 points) of signal is processed by FFT overlap for both signals received by H_1 and H_2. According to Figure 17, the results show that the maximum amplitude ($N_{FFT, H1}$) is located at 169 whereas the maximum amplitude ($N_{FFT, H2}$) is located at 174. The distance measurements are calculated as shown in Figure 18. The result clearly shows that the position of the target can be estimated by using equations (7) and (8) correctly.

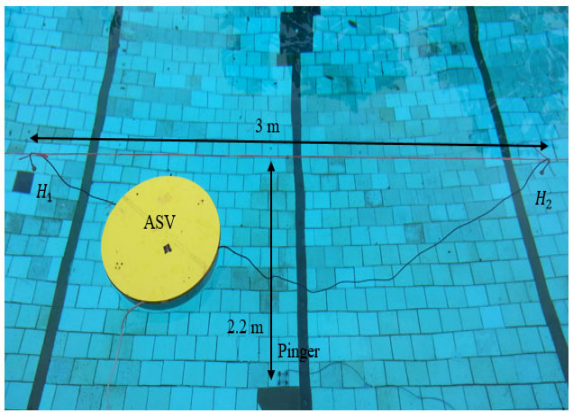

Fig. 16 — Experimental set-up of position estimation in pool

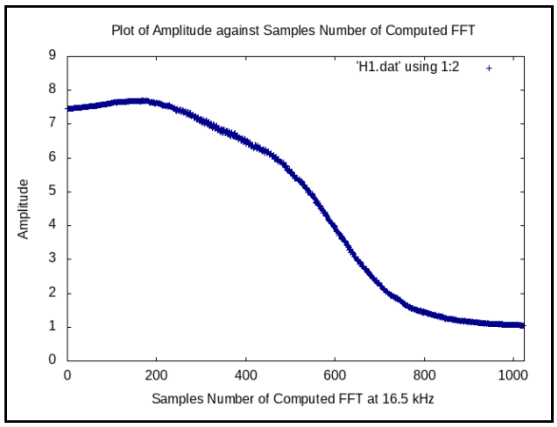

(a)

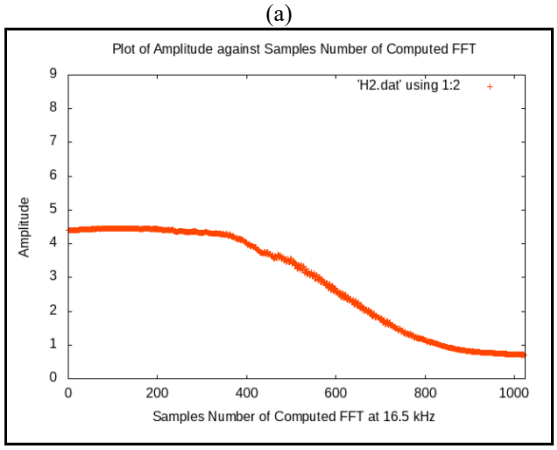

(b)

Fig. 17 — Experimental results of FFT overlap at 16.5 kHz (a) Signal received from left hydrophone and (b) Signal received from right hydrophone

Figure 19 shows that the actual location of target is at (x=1.5, y=-2.2) m. Ten times of position estimation are repeated in this experiment. The result of TOA estimation with location of target is plotted as shown in Figure 19. The standard error distribution of the TOA positioning is 0.048, 0.069 m. As a result,

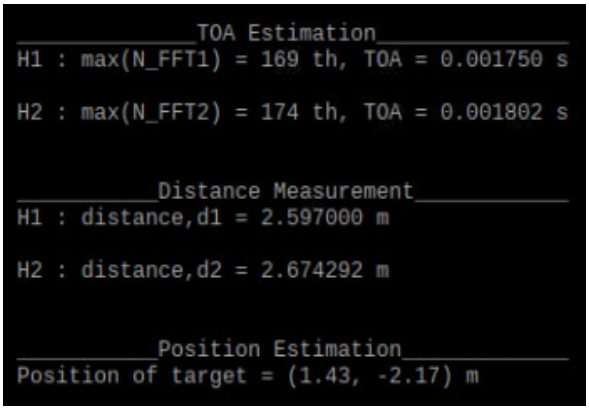

Fig. 18 — Experimental result of TOA estimation, distance measurement and position estimation

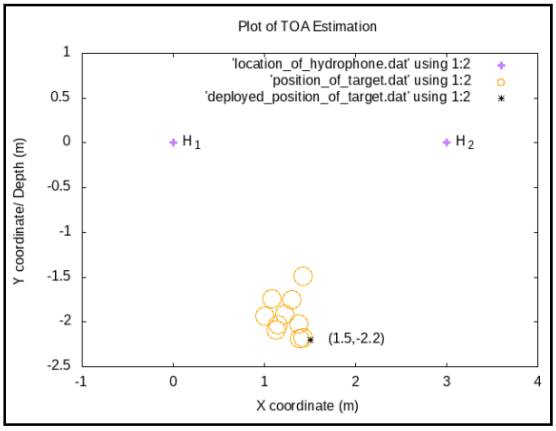

Fig. 19 — Experimental result of position estimation using proposed FFT overlap algorithm

the experimental result demonstrated that the position of target can be estimated correctly using proposed method (low-cost hardware platform and FFT overlap algorithm).

Conclusion

This paper proposed a low-cost underwater acoustic distance measurement by using FFT overlap. Pinger and hydrophone are designed by using piezoelectric element to reduce the cost. The hardware and software interfaces are implemented using low-cost hardware platform. This system also has low latency, low storage requirements and is cost-effective. Overall, the project approximately required an amount of USD 200 to come out with a complete platform. The cost is far below the cost of the commercially available product in the market which is USD 5000[30]. Of course, the performance may be different; however, the experimental results indicated that the proposed low-cost system still able to provide with accurate position estimation in a real environment.

In this paper, x-y location of target is estimated by using the proposed algorithm. The platform can be further tested by using three or more hydrophones in the wider water area as to determine 3D position of target. This will provide with more reliable data as to verify the efficacy of the developed platform. That will be the next experimental analysis conducted for this project.

Furthermore, the system also requires a robust TOA measurement to work well under different underwater environment. The FFT overlap algorithm can be improved by combining the received signal strength readings. The concept of this system can be further applied to multiple ASVs with better accuracy of global positioning system to perform underwater communication. Hence, the proposed system can be installed for future work such as underwater obstacle avoidance, positioning system and tracking system.

Acknowledgment

This project is supported by the FRGS Grant: 203/PELECT/6071291. The authors would like to thank Universiti Sains Malaysia for providing necessary tools and instrumentation to conduct the research. The permission given especially during the experimental testing is truly appreciated.

References

1 Kuperman, W. & Roux, P., Underwater Acoustics, In T. Rossing (eds) Springer Handbook of Acoustics, New York: Springer, 2007.

2 Lurton, X., An introduction to underwater acoustics: Principles and applications, 2nd Eds., London: Springer, 2010.

3 Arshad, M.R., Recent advancement in sensor technology for underwater applications, Indian J. Mar. Sci., vol. 38, no. 3, pp. 267-273, 2009.

4 Majid, M. H. A. & Arshad, M. R., Underwater acoustic source localization strategy by a group of autonomous surface vehicles, in Proceedings of the IEEE International Conference on Underwater System Technology: Theory & Applications, pp. 26-31, 2016.

5 Sasano, M., Inaba, S., Okamoto, A., Seta, T., Tamura, K., Ura, T., Sawada, S. & Suto, T., Development of a regional underwater positioning and communication system for control of multiple autonomous underwater vehicles, in Proceedings of the IEEE International Conference on Autonomous Underwater Vehicles, pp. 431-434, 2016.

6 Choi, H., Woo, J. & Kim, N., Localization of an underwater acoustic source for acoustic pinger-based transit in 2016 Maritime RobotX Challenge, IEEE Underwater Technology, 21-24 Feb, Busan South Korea, pp. 1-7, 2017.

7 Du, L., Chen, W. & Xie, T., Design of underwater ultrasonic distance measurement using in arctic sea ice monitoring with

high precision, 7th Int. Conf. on Information Science and Technology, 16-19 Apr, Da Nang, Vietnam, pp. 411-415, 2017.
8 Galarza, C., Masmitja, I., Prat, J. & Gomàriz, S., Design of obstacle detection and avoidance system for Guanay II AUV, in Proceedings of the 24th Mediterranean Conference on Control and Automation, pp. 410-414, 2016.
9 Kleeman, L. & Kuc, R., Sonar sensing, Springer Handbook of Robotics, pp. 491-519, 2008.
10 Zhou, Y., Song, A. & Tong, F., Underwater acoustic channel characteristics and communication performance at 85 kHz, J. pf Acoustical Society of America, 142(4):1-6, 2017.
11 Diamant, R., Kastner, R. & Zorzi, M., Detection and time-of-arrival estimation of underwater acoustic signals, IEEE 17th Int. Workshop on Signal Processing Advances in Wireless Communications, 3-6 Jul, Edinburgh, UK, pp. 1-5, 2016.
12 Biao W & Cheng H, Underwater target direction of arrival estimation by small acoustic sensor array based on sparse Bayesian learning, Polish Maritime Research, 24(s2): 95-102, 2017.
13 Casey, T., Guimond, B. & Hu, J., Underwater vehicle positioning based on time of arrival measurements from a single beacon, in IEEE OCEANS 2007, pp. 1-8, 2007.
14 Valente, J. F. & Alves, J. C., Real-time TDOA measurements of an underwater acoustic source, MTS/IEEE Monterey Oceans, 19-23 Sept, Monterey CA, USA, pp. 1-7, 2016.
15 Abutalebi, H. R. & Momenzadeh, H., Performance improvement of TDOA-based speaker localization in joint noisy and reverberant conditions, EURASIP Journal on Advances in Signal Processing, vol. 2011, no. 621390, pp. 1-13, 2011.
16 Shome, S., On methods to improve time delay estimation for underwater acoustic source localization, Indian J. Geo-Marine Sci., vol. 44, pp. 237-244, 2015.
17 Kou, X. Q. & Gu, L. C., Research of Long Range Accurate Ranging Technology Based on Ultrasonic Sensor Measurement, Journal of Networks, vol. 9, no. 8, pp. 2161-2167, 2014.
18 Cai, Z., Mohlenhoff, J. & Puklavage, C., Acoustic pinger locator subsystem, Senior Design Report, Univ. of Central Florida, 2009.
19 NOAA, What is a hydrophone? National Ocean Service Website, https://oceanservice.noaa.gov/facts/hydrophone.html Accessed on 15/07/18.
20 Sherman, C. H. & Butler, J. L., Transducers and Arrays for Underwater Sound, New York: Springer, 2007.
21 Li, H., Deng, Z. D. & Carlson, T. J., Piezoelectric Materials Used in Underwater Acoustic Transducers, Sensor Letters, vol. 10, no.3/4, pp. 679-697, 2012.
22 Benson, B., Li, Y., Kastner, R., Faunce, B., Domond, K., Kimball, D. & Schurgers, C., Design of a low-cost, underwater acoustic modem for short-range sensor networks, in Proceedings of the IEEE OCEANS 2010, Sydney, Australia, pp. 1-9, 2010.
23 Hu, F., Xiao, Y., Tilghman, P., Mokey, S., Byron, J. & Sackett, A., HW/SW Co-Design of a Low-Cost Underwater Sensor Node with Intelligent, Secure Acoustic Communication Capabilities, Underwater Acoustic Sensor Network, CRC Press, pp. 269-292, 2010.
24 Arunan, A. & Aryadevi, R. D., Design of wireless sensor network for submarine detection, Advances in Intelligent Systems and Computing, vol. 394, pp. 135-149, 2016.
25 Collins, N., Amplification and Distortion: A Simple Circuit That Goes from Clean Preamp to Total Distortion, Handmade Electronic Music: The Art of Hardware Hacking, 1st ed., New York: Taylor & Francis, pp. 151-156, 2009.
26 Newmarch, J., Sound Codes and File Formats, Linux Sound Programming, 1st ed., Berkeley, CA: Apress, pp. 11-14, 2017.
27 Vaingast, S., Science and Visualization, Beginning Python Visualization: Crafting Visual Transformation Scripts, 2nd ed., Berkeley, CA: Apress, pp. 269-306, 2014.
28 Heideman, M. T., Johnson, d. H. and Burrus, C. S., Gauss and the history of the fast Fourier transform, IEEE ASSP Magazine, vol. 1, no. 4, pp. 14-21, 1984.
29 Klungmontri, C., Nilkhamhang, I., Covanich, W. & Isshiki, T., Underwater positioning systems for underwater robots using trilateration algorithm, in Proceedings of the 6th IEEE International Conference on Information and Communication Technology for Embedded Systems (IC-ICTES), Hua-Hin, Thailand, pp. 1-5, 2015.
30 Stojanovic, M., Beaujean, P., Dhanak, M. R., Xiros, N. I. & Curtin, T., Acoustic communication, Springer Handbook of Ocean Engineering, Cham, Switzerland: Springer, pp. 359-386, 2016.